JACS
JOURNAL OF THE AMERICAN CHEMICAL SOCIETY
Article
pubs.acs.org/JACS

# Hydride in $BaTiO_{2.5}H_{0.5}$: A Labile Ligand in Solid State Chemistry

Naoya Masuda,[†] Yoji Kobayashi,[*,†,‡] Olivier Hernandez,[§] Thierry Bataille,[§] Serge Paofai,[§] Hajime Suzuki,[†] Clemens Ritter,[⊥] Naoki Ichijo,[∥] Yasuto Noda,[∥] Kiyonori Takegoshi,[∥] Cédric Tassel,[†] Takafumi Yamamoto,[†] and Hiroshi Kageyama[*,†,#]

[†]Department of Energy and Hydrocarbon Chemistry, Graduate School of Engineering, Kyoto University, Nishikyo-ku, Kyoto 615-8510, Japan

[‡]PRESTO, Japan Science and Technology Agency (JST), Kawaguchi-shi, Saitama 332-0012, Japan

[§]Institut des Sciences Chimiques de Rennes, UMR CNRS 6226, Université de Rennes 1, Bâtiment 10B, Campus de Beaulieu, Rennes F-35042, France

[⊥]Institut Laue-Langevin, 6, rue Jules Horowitz, Grenoble 38000, France

[∥]Department of Chemistry, Graduate School of Science, Kyoto University, Sakyo-ku, Kyoto 606-8502, Japan

[#]CREST, Japan Science and Technology Agency (JST), Kawaguchi-shi, Saitama 332-0012, Japan

Supporting Information

**ABSTRACT:** In synthesizing mixed anion oxides, direct syntheses have often been employed, usually involving high temperature and occasionally high pressure. Compared with these methods, here we show how the use of a titanium perovskite oxyhydride ($BaTiO_{2.5}H_{0.5}$) as a starting material enables new multistep low temperature topochemical routes to access mixed anion compounds. Similar to labile ligands in inorganic complexes, the lability of $H^-$ provides the necessary reactivity for syntheses, leading to reactions and products previously difficult to obtain. For example, $BaTiO_{2.5}N_{0.2}$ can be prepared with the otherwise inert $N_2$ gas at 400−600 °C, in marked contrast with currently available oxynitride synthetic routes. $F^-/H^-$ exchange can also be accomplished at 150 °C, yielding the oxyhydride-fluoride $BaTi(O, H, F)_3$. For $BaTiO_{2.4}D_{0.3}F_{0.3}$, we find evidence that further anionic exchange with $OD^-$ yields $BaTiO_{2.4}(D^-)_{0.26}(OD^-)_{0.34}$, which implies stable coexistence of $H^+$ and $H^-$ at ambient conditions. Such an arrangement is thermodynamically unstable and would be difficult to realize otherwise. These results show that the labile nature of hydride imparts reactivity to oxide hosts, enabling it to participate in new multistep reactions and form new materials.

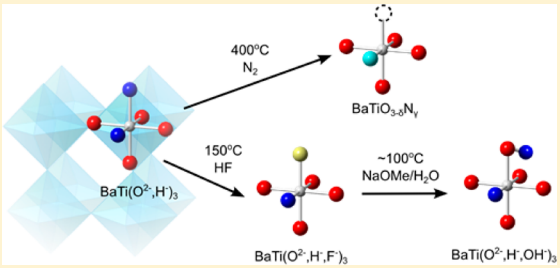


## INTRODUCTION

Over the years, a large number of mixed anion transition metal oxides, such as oxynitrides,[1] oxyfluorides,[2] and oxysulfides[3] with appealing properties have been reported. A relatively new addition to this family of mixed anion oxides are the oxyhydrides, where anionic hydrogen ($H^-$) coexists with $O^{2-}$. Examples of transition metal oxyhydrides are $LaSrCoO_3H_{0.7}$,[4] (Ba, Ca, Sr)$TiO_{2.5}H_{0.5}$,[5,6] and very recently $SrVO_2H$,[7] $Sr_2VO_3H$,[8] and $SrCrO_2H$.[9] For $LaSrCoO_3H_{0.7}$, a previous study using quasi-elastic neutron scattering reports that the hydride mobility is quite high at about 400 °C.[10]

In our own studies with $BaTiO_{2.4}H_{0.6}$, we find facile H/D exchange at 400 °C when the oxyhydride is exposed to a $D_2$ atmosphere.[5] Compared to $O^{2-}$ diffusion in oxides, $H^-$ within an oxide lattice can be expected to be quite mobile, given its light mass and low electrostatic charge. The hydride is also *thermolabile*, i.e., when heated to high temperatures (ca. 400 °C) under inert atmosphere, oxyhydrides release the hydride as $H_2$ gas, with a highly anion-deficient structure (such as $BaTiO_{2.4}\square_{0.6}$) presumed to result initially before its inadvertent oxidation.[5]

This concept of hydride lability in solid transition metal oxyhydrides has implications for synthesis in solid state chemistry. In coordination chemistry (i.e., solution phase), a diverse range of complexes is synthesized by ligand exchange, starting from precursor complexes with labile ligands. On the other hand, the solid state chemistry of oxides represents a different case, as the high lattice enthalpy between $O^{2-}$ and metal cations makes ligand (or anion) exchange possible at only very high temperatures. For example, the preparation of oxynitrides from oxides usually required high temperatures and strongly reducing conditions, such as the use of ammonia at 900−1000 °C.[11−13] However, we have recently shown that if an oxyhydride precursor ($BaTiO_{2.4}H_{0.6}$) is used, then the $NH_3$ reaction temperature can be lowered to 400−500 °C, while still achieving a high N content ($BaTiO_{2.4}N_{0.4}$).[14]

In this paper, we take this idea further and explore the synthetic scope of this oxyhydride precursor, as shown in the lower portion of Figure 1. We find that reacting the oxyhydride

**Received:** October 12, 2015
**Published:** November 17, 2015





DOI: 10.1021/jacs.5b10255
J. Am. Chem. Soc. 2015, 137, 15315−15321

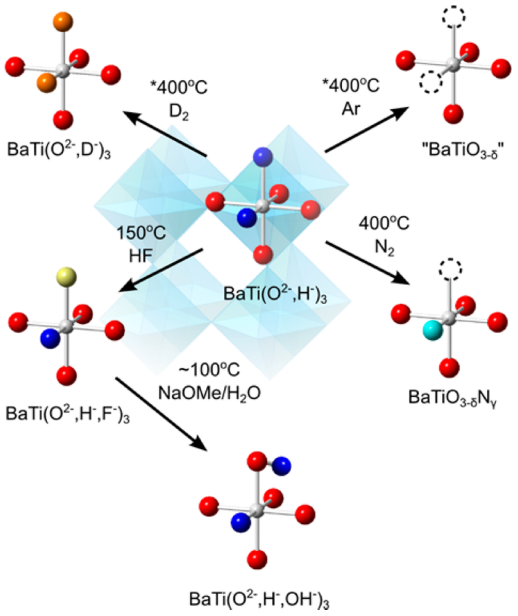


**Figure 1.** Studied anion exchange routes, starting from $BaTiO_{2.5}H_{0.5}$. The upper two routes (marked by an asterisk) to $BaTi(O,D)_3$ and $BaTiO_{3-\delta}$ were previously reported;[5] in this paper, we describe the lower reactions. The $O^{2-}$ and $H^-$ anions are shown by the red and blue spheres. $N^{3-}$ and $F^-$ are shown in light blue and light yellow, respectively.

with $N_2$ gas at moderate temperatures (400−600 °C) also leads to the formation of an oxynitride ($BaTiO_{2.5}N_{0.2}$), despite the usually inert nature of $N_2$. Hydride is also prone to reactions with oxidizing agents and acids, making other anion exchange possible. Hence, we also treated the oxyhydride with the acidic gas HF at 150 °C to obtain the mixed $BaTi(O, H, F)_3$ and $BaTi(O, F)_3$ compositions, the latter of which normally requires high pressure synthesis to be obtained.[15] The oxyhydride-fluoride is a convenient intermediate for the further exchange of the $F^-$ by $OH^-$ to prepare $BaTi(O^{2-}, H^-, OH^-)_3$, which contains hydrogen in both hydride and proton forms, which is quite surprising considering the inherent difficulty of avoiding an acid−base reaction between the two species.

## EXPERIMENTAL SECTION

**$BaTiO_{2.5}H_{0.5}$.** A polycrystalline sample of $BaTiO_{2.5}H_{0.5}$ was synthesized by the $CaH_2$ reduction of $BaTiO_3$ as reported previously.[5] Commercial powders of $BaTiO_3$ with average particle sizes of 100 nm (and 300 nm when noted) were used; TEM images are in the Supporting Information (SI). $BaTiO_3$ and $CaH_2$ were mixed in a $N_2$-filled glovebox (1:3 molar ratio); then pelletized (1.5 g, diameter 12 mm) and heated at 560 °C for 1 week in an evacuated (~$10^{-2}$ Pa) Pyrex tube (O.D. 20 mm, I.D. 14 mm, length approximately 12 cm). The blue-black $BaTiO_{2.5}H_{0.5}$ was obtained after washing with $NH_4Cl$/methanol (0.1 M, 300 mL) and drying at 100 °C under vacuum.

As in our previous studies,[5,6] the amount of hydride in the sample can be determined by a number of experimental methods, such as TGA (oxidative atmosphere), Rietveld refinement of X-ray data, thermal desorption spectroscopy (TDS), and if available, neutron diffraction. All techniques give a consistent formula, and the amount of anion vacancies is negligible.

**$BaTiO_{2.5}N_{0.2}$ ($H^-/N^{3-}$ Exchange).** A portion of $BaTiO_{2.5}H_{0.5}$ (0.1 g, ~100 nm particle size) was heated under $N_2$ flow (100 mL/min). Ramp rates of 5 °C/min (heating) and 10 °C/min (cooling) were used. Samples treated at 400 °C were held for 30 min., while samples treated at 600 °C were held for 5 min at the maximum temperature. Elevated pressure (5 atm) during $N_2$ flow was achieved by a back pressure regulator installed downstream. The nitrogen content was determined by combustion analysis.

**$BaTiO_{2.5}H_{0.25}F_{0.25}$. ($H^-/F^-$ Exchange).** $BaTiO_{2.5}H_{0.5}$ (0.05 g, 0.22 mmol ~300 nm particle size) was mixed with $NH_4F$ (CAUTION! 4.1 mg, 0.11 mmol) in a $N_2$-filled glovebox. The mixture was then placed in a 1/4 inch PTFE tube and sealed on both ends with Teflon Swagelok fittings. This tube was heated at 150 °C for 1 day to yield the product. The fluorine content was measured by combustion analysis/aqueous extraction followed by ion chromatography (Analytical Services, School of Pharmacy, Kyoto University).

**$BaTi(O^{2-}, H^-, OH^-)_3$ ($F^-/OH^-$ Exchange).** $BaTiO_{2.4}D_{0.3}F_{0.3}$ was prepared by reacting $BaTiO_3$ (~300 nm) with $CaD_2$ at 580 °C for 1 week, and then fluorinating with $NH_4F$ as described above. The preparation of $CaD_2$ is described in the SI. A portion of $BaTiO_{2.4}D_{0.3}F_{0.3}$ (1 g, 4.4 mmol) was suspended in 100 mL of NaOMe/$D_2O$ (0.54 g of NaOMe, pH = 13), purged with Ar, and then sealed in a Teflon vessel. The vessel was heated moderately on a hot plate for 4 days (hot plate set to 230 °C, Teflon container interior estimated at ~100 °C). After cooling to room temperature, the powder was washed with $D_2O$ and acetone under a $N_2$ atmosphere, and dried at 100 °C. Despite precautions to avoid atmospheric moisture, a preliminary neutron diffraction experiment showed substantial $^1H$ content; hence, an additional pure $D_2O$ treatment/wash was conducted before the final neutron diffraction measurement.

**Synchrotron X-ray Diffraction.** Powder samples were packed in 0.2 mm or 0.5 mm Lindemann glass capillaries, and mounted on a Debye−Scherrer camera at beamline BL02B2 at SPring-8 (JASRI). The diffraction patterns were recorded on imaging plates, and digitized with a step size of 0.01°. Rietveld refinements were conducted by the RIETAN[16] and FULLPROF[17] programs.

**Neutron Diffraction/MEM Analysis.** A powder sample was packed in a vanadium can under He atmosphere. Data were collected at room temperature on the D2B high resolution diffractometer at ILL (Grenoble, France). Due to the small unit cell and the high symmetry of the investigated crystal structure, a short wavelength of 1.05 Å was used in order to optimize the accessible $Q$-range without peak strong

**Table 1. Compositions of Oxynitrides Formed by Treatment of $BaTiO_{3-x}H_x$ with $N_2$ Gas**

| precursor[a] oxyhydride (Rietveld refinement) | $N_2$ pressure (atm) | temp. (°C) | composition[b] (Rietveld refinement) | composition[b] (elemental analysis) | space group, lattice parameter ($a$, $c$) |
|---|---|---|---|---|---|
| $BaTiO_{2.51(1)}H_{0.49(1)}$[c] | 1 | 300 | $BaTiO_{2.49(1)}$ | $BaTiO_{2.49}N_0$ | *Pm*-3*m*, 4.030005(4) Å |
| $BaTiO_{2.51(1)}H_{0.49(1)}$[c] | 1 | 400 | $BaTi(O,N)_{2.84(1)}$ | $BaTiO_{2.51}N_{0.15}$ | *P*4*mm*, 4.01600(8) Å, 4.0238(1) Å |
| $BaTiO_{2.51(1)}H_{0.49(1)}$[c] | 1 | 600 | $BaTi(O,N)_{2.85(1)}$ | $BaTiO_{2.51}N_{0.23}$ | *P*4*mm*, 4.0125(1) Å, 4.0184(2) Å |
| $BaTiO_{2.71(1)}H_{0.29(1)}$[d] | 5 | 600 | $BaTi(O,N)_{2.94(2)}$ | $BaTiO_{2.71}N_{0.21}$ | *P*4*mm*, 4.0110(4) Å, 4.0133(8) Å |
| $BaTiO_{2.51(1)}H_{0.49(1)}$[c] | 5 | 600 | $BaTi(O,N)_{2.95(1)}$ | $BaTiO_{2.51}N_{0.27}$ | *P*4*mm*, 4.0126(2) Å, 4.0184(2) Å |

[a]H content based on assumption of full occupancy. [b]H content not explicitly determined, hence not shown. [c]*Pm*-3*m*, $a$ = 4.02995(4) Å. [d]*Pm*-3*m*, $a$ = 4.01132(3) Å.



DOI: 10.1021/jacs.5b10255
J. Am. Chem. Soc. 2015, 137, 15315−15321

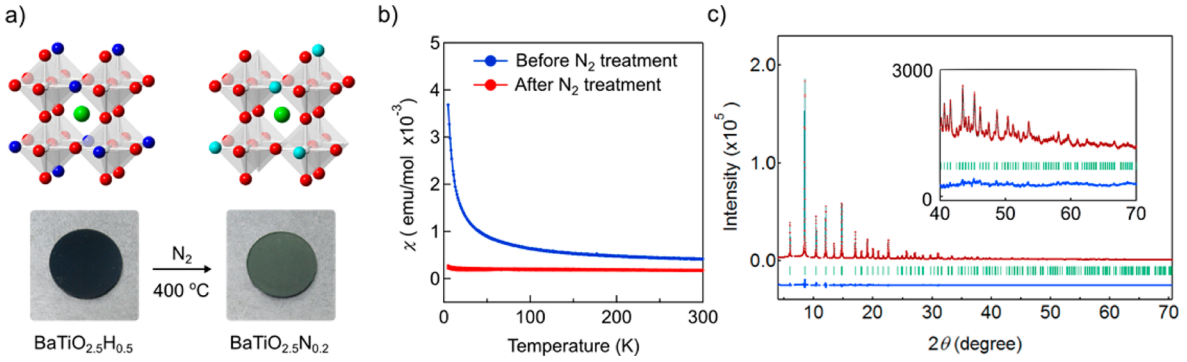


**Figure 2.** (a) Colors of samples before and after treatment with $N_2$ at 400 °C under 1 atm, (b) magnetic susceptibilities of the sample before and after nitridation, and (c) Rietveld refinement of synchrotron X-ray diffraction data of the oxynitride sample ($\lambda$ = 0.42044 Å); the inset shows a magnified view of the higher angle region. Small impurity peaks (~1% intensity) have been excluded.

**Table 2. Structural Parameters from Rietveld Refinements of $BaTiO_{2.5}H_{0.5}$, $BaTiO_{2.5}N_{0.2}$, and $BaTiO_{2.5}H_{0.25}F_{0.25}$. (Synchrotron X-ray powder diffraction data.)**

| compound | atom | site | $x/a$ | $y/b$ | $z/c$ | occ. | $100U_{iso}$ (Å$^2$) |
|---|---|---|---|---|---|---|---|
| $BaTiO_{2.5}H_{0.5}$[a] | Ba | 1*b* | 0.5 | 0.5 | 0.5 | 1 | 0.646(6) |
| *Pm*-3*m* | Ti | 1*a* | 0 | 0 | 0 | 1 | 1.03(4) |
| *a* = 4.02995(4) Å | O/H | 3*d* | 0.5 | 0 | 0 | 0.837(3) | 1.18(4) |
| | | $R_{wp}$ = 4.43%, $R_p$ = 3.36%, $\chi^2$ = 5.56, $R_B$ = 1.99%, $R_F$ = 1.64% | | | | | |
| $BaTiO_{2.5}N_{0.2}$ | Ba | 1*b* | 0.5 | 0.5 | 0.5 | 1 | 0.64(1) |
| *P*4*mm* | Ti | 1*a* | 0 | 0 | −0.025(2) | 1 | 0.72(9) |
| *a* = 4.0126(1) Å | O1/N1 | 1*a* | 0 | 0 | −0.486(6) | 0.949(3)[c] | 0.69(5)[c] |
| *a* = 4.0184(2) Å | O2/N2 | 2*c* | 0 | 0.5 | 0.011(4) | 0.949(3)[c] | 0.69(5)[c] |
| | | $R_{wp}$ = 3.92%, $R_p$ = 2.95%, $\chi^2$ = 4.41, $R_B$ = 3.18%, $R_F$ = 1.87% | | | | | |
| $BaTiO_{2.5}H_{0.5}$[b] | Ba | 1*b* | 0.5 | 0.5 | 0.5 | 1 | 0.521(7) |
| *Pm*-3*m* | Ti | 1*a* | 0 | 0 | 0 | 1 | 1.09(1) |
| *a* = 4.02085(3) Å | O/H | 3*d* | 0.5 | 0 | 0 | 0.839(4) | 1.47(6) |
| | | $R_{wp}$ = 6.20%, $R_p$ = 4.49%, $\chi^2$ = 8.82, $R_B$ = 2.71%, $R_F$ = 1.34% | | | | | |
| $BaTiO_{2.5}H_{0.25}F_{0.25}$[d] | Ba | 1*b* | 0.5 | 0.5 | 0.5 | 1 | 0.406(3) |
| *Pm*-3*m* | Ti | 1*a* | 0 | 0 | 0 | 1 | 1.02(1) |
| *a* = 4.01489(4) Å | O/F/H | 3*d* | 0.5 | 0 | 0 | 0.912(4) | 1.37(5) |
| | | $R_{wp}$ = 4.37%, $R_p$ = 3.13%, $\chi^2$ = 4.71, $R_B$ = 2.44%, $R_F$ = 0.85% | | | | | |

[a]Precursor (particle size ~ 100 nm) used for the synthesis of $BaTiO_{2.5}N_{0.2}$. [b]Precursor (particle size ~ 300 nm) used for the synthesis of $BaTiO_{2.5}H_{0.25}F_{0.25}$. [c]Occupancies and $U_{iso}$ values for O1/N1 and O2/N2 were constrained to each other. [d]Assumed formula.

peak overlap. For the $BaTi(O^{2-}, D^-, OD^-)3$ sample, the data was first refined (RIETAN) based on a cubic $BaTiO_{3-x}D_x$ model without including any interstitial $D^+$ atoms of the $OD^-$ hydroxyl groups. Using as *F*-constraints the structure factors extracted from the Rietveld refinement, a maximum entropy method (MEM) analysis was carried out. Then REMEDY cycles, including MEM-based whole pattern fitting, were conducted through the combined use of PRIMA[18] and RIETAN. Nuclear densities from final MEM analysis were visualized by the program VESTA.[19]

## RESULTS AND DISCUSSION

**An Oxynitride from $N_2$: $BaTiO_{2.5}N_{0.2}$.** $BaTiO_{2.85}N_{0.1}$ has already been synthesized previously by treating $BaTiO_3$ with $NH_3$ at 950 °C,[12] and more recently from $BaTiO_{2.4}H_{0.6}$ with $NH_3$ at 400−500 °C.[14] Here, we heated a sample of $BaTiO_{2.5}H_{0.5}$ under flowing $N_2$ gas at various temperatures and pressures (1−5 atm, 300−600 °C) as shown in Table 1. After the reaction (above 300 °C), the blue-black sample became green (Figure 2a), indicating a Ti oxidation state of primarily $Ti^{4+}$, with a trace amount of reduced sites. The magnetic susceptibility data (Figure 2b) show that $Ti^{4+}$, rather than the original paramagnetic $Ti^{3.5+}$ is present. Elemental analysis of the collected powders shows a substantial nitrogen content ranging up to 1.82 wt%, corresponding to the formulas shown in Table 1.

Synchrotron XRD patterns (Figure 2c) on the $N_2$-treated powders show no known nitride impurity phases, so the nitrogen should be incorporated into the barium titanate lattice. The diffraction patterns indicate a tetragonal structure with $c/a > 1$. This is consistent with the loss of conducting electrons and a second-order Jahn−Teller effect as in $BaTiO_3$. We confirm the anion composition by comparing the XRD Rietveld refinement results of oxyhydride precursors and $N_2$-treated samples. Oxygen and nitrogen are indeed indistinguishable by XRD, but with respect to the oxyhydride precursor, the apparent anion occupancy (O/N) should increase. For example, by Rietveld refinement of XRD data, the precursor $BaTiO_{2.51}H_{0.49}$ appears to be "$BaTiO_{2.51}$", whereas after being treated by flowing $N_2$ at 400 °C, the apparent composition becomes $BaTi(O/N)_{2.84}$. The remaining results of the refinement are shown in Table 2. Assuming the $N_2$ flow has no $O_2$ impurity, we may assume that the increase in anion occupancy is from nitrogen only, implying a composition of $BaTi^{4+}O_{2.51}N_{0.33}$. The elemental analysis result is **1.10** wt% ($BaTiO_{2.51}N_{0.15}$), a slight underestimation. We have also checked for the presence of remaining hydride in selected


DOI: 10.1021/jacs.5b10255
J. Am. Chem. Soc. 2015, 137, 15315−15321

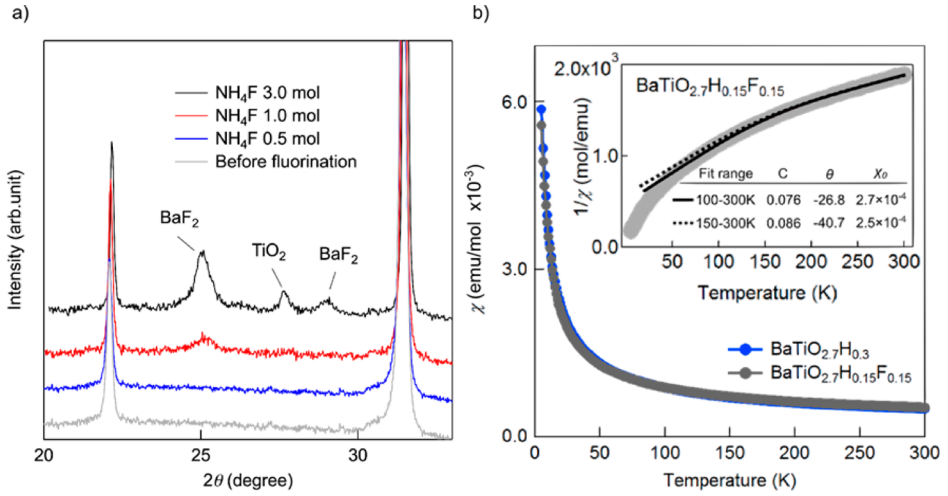


**Figure 3.** (a) Raw XRD pattern of $BaTiO_{2.5}H_{0.5}$ treated with various equivalents of $NH_4F$, and (b) Magnetic susceptibility data (0.1 T) of the oxyhydride before and after fluorination. The inset shows the Curie–Weiss fits of the fluorinated product at over two different temperature ranges. Units of $C$, $\theta$, and $\chi$ are emu·K·mol$^{-1}$, K, and emu·mol$^{-1}$, respectively.

samples (those treated at 600 °C) by TDS, but found no remaining hydride. There is some disagreement between the anion compositions determined by Rietveld refinements and elemental analysis, perhaps due to $O_2$ impurities in the $N_2$ gas stream. However, in general, oxynitrides of substantial nitrogen content (tentative formula ≈ $BaTiO_{2.5}N_{0.2}$) can be prepared under very mild conditions using $N_2$ gas, similar to our recent work with $NH_3$.[14]

This reactivity between our oxyhydrides and $N_2$ gas at moderate temperature is quite unusual, given the inert nature of $N_2$ due to the strong N≡N bond. Some oxynitrides such as spinel-type aluminum oxynitrides[20] and $Nd_2AlO_3N$[21] have been synthesized with $N_2$ gas in the presence of a reducing agent such as carbon or CO, but only at extremely high temperatures (1200–1600 °C). The synthesis of full metal nitrides with $N_2$ at low temperatures is also rather rare, except for certain alkali or alkali earth metals such as Li (exothermic reaction at ∼150 °C)[22] and Mg (∼600 °C).[23] Titanium metal itself typically requires heating above 800 °C to form various nitrides.[24] The surprisingly low temperature for the nitridation of the oxyhydride (400 °C) here is due to the thermolability of $H^-$, such that $BaTiO_{2.5}H_{0.5}$ would otherwise transform to $BaTiO_{2.5}\square_{0.5}$ when the hydride leaves. The Ti cation becomes coordinatively highly unsaturated, and in its activated state cleaves the N≡N bond and forms the oxynitride. In the usual $NH_3$ treatment of oxides, the $O^{2-}$ anion is removed by the reducing environment of the $H_2$ created in situ by the decomposition of $NH_3$. In our case, one can think of the $O^{2-}$ anion removed by the strong reducing power of $CaH_2$ during oxyhydride formation (500–560 °C), followed by subsequent reaction with $N_2$. Given the low overall processing temperature (max. 560 °C) and the various new oxyhydrides reported recently, oxyhydrides may be an attractive route to synthesize new oxynitrides in nanomaterial form.

**Synthesis of Oxyhydride-Fluorides and Oxyfluorides, $BaTi(O^{2-}, H^-, F^-)_3$.** Other than the thermolability of $H^-$, we also examine the reactivity of $H^-$ with acids in order to perform anion exchange. If $BaTiO_{2.5}H_{0.5}$, which contains $H^-$, were to be reacted with a Brønsted acid such as HF, then the following acid–base reaction should result:

$$BaTiO_{2.5}H_{0.5} + 0.5HF \rightarrow [BaTiO_{2.5}\square_{0.5} + 0.5H_2 + 0.5F^-] \quad (1)$$

$$[BaTiO_{2.5}\square_{0.5} + 0.5F^-] \rightarrow BaTiO_{2.5}F_{0.5} \quad (2)$$

The final fluorine content should largely be determined by the initial amount of hydride present, and if substoichiometric quantities of HF were reacted, oxyhydride-fluorides should result. Due to the hazardous nature of handling HF gas in the laboratory, we sealed a powder sample of $BaTiO_{2.5}H_{0.5}$ with a calculated amount of $NH_4F$ in a Teflon tube under $N_2$ atmosphere. The tube was then heated to 150 °C, where $NH_4F$ decomposes to $NH_3$ and HF. At this temperature, $NH_3$ seems not to react with oxyhydride, but HF readily reacts.

The reaction does not result in any color change, but XRD shows formation of $BaF_2$ when more than 1 equivalent (per $H^-$) of $NH_4F$ is used (Figure 3a). When 0.5 equivalents of $NH_4F$ are reacted, elemental analysis and EDX show the presence of fluorine (2.2(1) wt%). Similar to the $BaTiO_{2.5}N_{0.2}$ case mentioned above, we also examined the anion composition by Rietveld refinement of synchrotron X-ray diffraction data. The initial $BaTiO_{2.51}H_{0.49}$ refines to "$BaTiO_{2.51}$", whereas after fluorination with 0.5 mol equivalents (per $H^-$) of $NH_4F$, the apparent composition is "$BaTi(O, F)_{2.74}$". The fluorine content from elemental analysis (2.2 wt%) implies a formula of $BaTiO_{2.51}F_{0.26}$, which agrees well with the Rietveld result. Hence, the fluorine is probably distributed throughout the particle as opposed to simply on the surface. On the basis of our previous experience with $BaTiO_{3-x}H_x$ generally not exhibiting any appreciable amount of anion vacancies, we suspect the final formula to be $BaTiO_{2.5}F_{0.25}H_{0.25}$. The slight decrease in lattice parameter may be due to the different anionic radii. For the fluorination of a slightly different sample ($BaTiO_{2.7}H_{0.3}$ with 0.5 eq. $NH_4F$; Rietveld refinement results in the SI) we also obtained magnetization data, as shown in Figure 3b. The fluorination reaction has virtually no effect on the magnetization curve, indicating no change in Ti oxidation state. A Curie–Weiss fit of the data of the fluorinated sample (Figure 3b, inset) gives a Curie constant of 0.076 ∼ 0.086 emu·K·mol$^{-1}$, signifying an average Ti oxidation state of


DOI: 10.1021/jacs.5b10255
J. Am. Chem. Soc. 2015, 137, 15315–15321

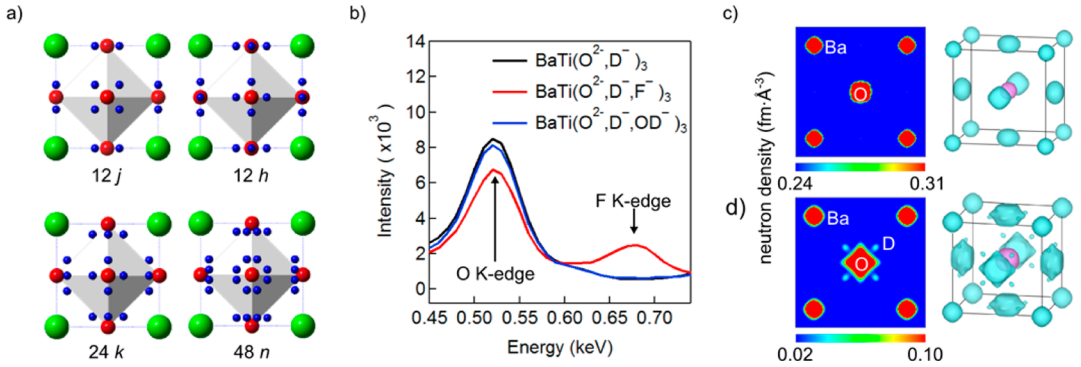


**Figure 4.** (a) Various possible distributions of interstitial protons in perovskites and their Wyckoff positions (12*j*, 12*h*, 24*k*, 48*n*). The Ba cation (green) is placed at the corner of the unit cell, oxygen (red) is at the corner of the $TiO_6$ octahedra, and interstitial proton is shown in blue. (b) EDX spectra of various samples, showing the presence/absence of fluorine (F *K*-edge at 0.677 eV). (c) 2-D and spatial MEM nuclear density maps of a $BaTiO_{2.4}D_{0.6}$ precursor sample before HF and NaOMe/$D_2O$ treatment and (d) after treatment. Difference in overall nuclear density levels possibly due to background from quartz container for (c).

**Table 3. Structural Parameters from Rietveld Refinement of Synchrotron X-ray and Neutron Diffraction Patterns of $BaTiO_{2.4}D_{0.3}(OD)_{0.3}$.**

| | atom | site | *x*/*a* | *y*/*b* | *z*/*c* | occ. | $100U_{iso}$ (Å$^2$) |
|---|---|---|---|---|---|---|---|
| X-ray data | Ba | 1*b* | 0.5 | 0.5 | 0.5 | 1 | 0.867(5) |
| *Pm*-3*m* | Ti | 1*a* | 0 | 0 | 0 | 1 | 1.06(1) |
| *a* = 4.02768(2) Å | O | 3*d* | 0.5 | 0 | 0 | 0.91(1) | 1.674(9) |
| | $R_{wp}$ = 6.70%, $R_p$ = 5. 87%, $\chi^2$ = 4.99, $R_B$ = 1.60%, $R_F$ = 1.77% | | | | | | |
| neutron data | Ba | 1*b* | 0.5 | 0.5 | 0.5 | 1 | 0.64(8) |
| *Pm*-3*m* | Ti | 1*a* | 0 | 0 | 0 | 1 | 0.94(9) |
| *a* = 4.017(1) Å | O/D | 3*d* | 0.5 | 0 | 0 | 0.997(9) | 1.1(1)[a] |
| | D | 12*j* | 0.5 | 0.175(1) | 0.175(1) | 0.029(1) | 1.1(1)[a] |
| | $R_{wp}$ = 1.47%, $R_p$ = 1.13%, $\chi^2$ = 2.72, $R_B$ = 2.96%, $R_F$ = 1.44% | | | | | | |

[a] $U_{iso}$ values were constrained to each other.

approximately + 3.65. All of these results indicate that a 1:1 $H^-/F^-$ exchange has occurred.

Rietveld refinement results for samples treated with increased amounts of $NH_4F$ (1 and 3 equiv) also showed an increased (O/F) occupancy ($(O/F)_{0.98}$ and $(O/F)_{0.99}$, respectively), and with formation of $BaF_2$ when more than 1 equiv. of fluorine is reacted. This trend, the agreement with elemental analysis, and the fact that $O_2$ was not present during the reaction point to our successful formation of a oxyhydride-fluoride at very mild conditions (150 °C). $BaTiO_{3-x}F_x$ has been previously reported, but its synthesis requires high pressure and high temperature (3 GPa, 1300 °C), and the authors report a maximum fluorine content of only $BaTiO_{2.9}F_{0.1}$.[15]

**Coexisting $H^-$ and $H^+$: $BaTi(O^{2-}, H^-, OH^-)_3$.** The $BaTi(O^{2-}, H^-, F^-)_3$ system serves as a convenient stepping stone for further anion exchange to yield more unprecedented compounds. The replacement of $F^-$ by $OH^-$ in (K, Ba)Ti(O, $F)_3$ single crystals has been accomplished by simply heating with $H_2O$ or $D_2O$ under hydrothermal conditions (230 °C), or even at ambient conditions over extended periods of time.[25] We decided to perform this exchange on $BaTiO_{2.4}H_{0.3}F_{0.3}$, since if no other side reactions occur, the presumed product would be $BaTiO_{2.4}H_{0.3}(OH)_{0.3}$. If synthesized, this compound would be a surprising case where $H^-$ and $OH^-$, or namely $H^-$ and $H^+$, coexist within the same crystal lattice. Thermodynamically, this is obviously a highly unfavorable arrangement, making it difficult to achieve by normal means.

For this study, we synthesized the deuterated version, starting from $BaTiO_{2.4}D_{0.6}$ and aimed for a final target composition of $BaTiO_{2.4}D_{0.3}(OD)_{0.3}$ through the $BaTiO_{2.4}D_{0.3}F_{0.3}$ oxyhydride fluoride. The smaller incoherent scattering cross section of deuterium when compared to hydrogen (2.05 barn vs 80.27 barn) yields a better signal-to-noise ratio, thus enhancing the contrast of potential hydroxyl groups hunted in the nuclear density maps reconstructed through the maximum entropy method (MEM) analysis from neutron powder diffraction data. This method has been used to study various perovskite proton conductors, and we expect the deuterated hydroxyl groups to appear as interstitial deuterons at approximately 1 Å from anionic ($O^{2-}$, $D^-$) sites, with numerous possible arrangements as shown in Figure 4a.

The EDX spectra of the intermediate starting material $BaTiO_{2.4}D_{0.3}F_{0.3}$ is shown in Figure 4b. A fluorine K-edge peak observed at 0.677 keV disappears after treatment with NaOMe/$D_2O$, indicating the total loss of fluorine. The neutron powder diffraction pattern of this NaOMe/$D_2O$-treated $BaTiO_{2.4}D_{0.3}F_{0.3}$ sample was analyzed by MEM-based whole pattern fitting, and the nuclear density maps obtained at final convergence are shown in Figure 4c,d. For the sake of comparison, the nuclear density map of $BaTiO_{2.4}D_{0.6}$ (Figure 4c)—as determined according to the same kind of MEM-calculations—is shown on Figure 4d. After HF and NaOMe/$D_2O$ treatments, localized nuclear density close to the oxygen site (3*d*) is evidenced, which is not present in the map for $BaTiO_{2.4}D_{0.6}$ (Figure 4c). This additional nuclear density at 12*j* (0.5, 0.175(1), 0.175(1)) is located 0.99758 Å away from the oxygen site, a typical distance for OH groups.



DOI: 10.1021/jacs.5b10255
J. Am. Chem. Soc. 2015, 137, 15315−15321

Given this additional nuclear density, a model for Rietveld refinement was constructed with $D^+$ inserted at the interstitial 12*j* site. At the anionic site, both $O^{2-}$ and $D^-$ statistically coexist, but given their somewhat close neutron coherent scattering lengths (O: + 5.803 fm, D: + 6.671 fm), the site was tentatively modeled as an O pseudoatom. The refinement yielded chemical occupancies of 0.029(1) for $D^+$ and 0.997(9) for the anionic site (Table 3). Considering the multiplicities of each Wyckoff site, the formula unit from neutron data thus becomes $BaTi(O^{2-}/D^-)_{2.99(2)}\ D^+_{0.35(1)}$. We then turned to synchrotron X-ray diffraction data of the same sample, which is insensitive to deuterium, and allows us to refine the global oxygen composition only. A Rietveld refinement of the X-ray data gives the parameters shown in Table 3, and the formula $BaTiO_{2.73(3)}\square_{0.27(3)}$. The oxygen content here corresponds to the oxide ions plus the oxygen atoms of the hydroxide groups (i.e., $O_O$ and $OD_O^\bullet$ in Kröger-Vink notation), and the apparent vacancy can be reasonably assumed to be $D^-$ content. Altogether, the neutron and X-ray results agree on the formula $BaTiO_{2.4}D_{0.27}(OD)_{0.35(1)}$, which we rounded up to $BaTiO_{2.4}D_{0.26}(OD)_{0.34}$.

While hydroxyl groups can be identified by other techniques such as IR or NMR, MEM-computed nuclear density maps using neutron diffraction data as constraints are in principle a direct way to prove the existence of hydroxyl groups throughout the bulk of the crystallites as opposed to the surface. We could not gain good IR spectra perhaps due to dark color of the sample, and NMR is not simple given the paramagnetic nature of the sample and the ambiguity surrounding chemical shifts of $H^-$ and $H^+$.[26] However, on the basis of the absence of $F^-$ after $NaOMe/D_2O$ treatment and the nuclear density maps from neutron diffraction data, we believe these data show that our multistep anion exchange route starting from an oxyhydride has much potential to obtain various unusual compositions.

The determined $BaTiO_{2.4}D_{0.26}(OD)_{0.34}$ composition appears to be stable at room temperature for a few weeks or months, given the time elapsed between the synthesis and neutron diffraction experiment. We previously observed that $BaTiO_{2.5}H_{0.5}$ itself is stable in water,[5] which was also encouraging since water itself contains protonic hydrogen.

The suggested presence of $D^+$ at the 12*j* site is somewhat surprising, but may be related to the relative stability of this $H^+/H^-$ composition. Other proton conductors typically have interstitial protons at the 12*h* (0.5, *y*, 0), 24*k* (*x*, *y*, 0), and 48*n* (*x*, *y*, *z*) sites (Figure 4a).[27−30] The choice of site may be determined by various factors, such as B—O bonding, temperature, and $H^+$ concentration, but no other reports of occupancy at the 12*j* site have been found. The minimum distance between $D^+$ at the 12*j* site and $D^-$ is about 2.5 Å, which is slightly longer than the corresponding distances for the 12*h*, 24*k*, and 48*n* cases, so the arrangement probably offers the "most metastable" environment for the interstitial deuteron. In $NH_4Ca(BH_4)_3$, which is stable up to 100 °C, the protonic and hydridic species are separated by ∼2.2 Å.[31] In our case $O^{2-}/D^-$ mixing on the 3*d* site presumably further separates the proton-hydride distance, offering additional stability. It would be interesting to determine whether there are any clustering effects, affecting the $OD^-$ and $D^-$ arrangements—such anion−anion interactions are only possible in lattices containing three different species, and this issue has not been examined before.

Recently, a study by Hayashi et al. has shown with NMR and IR evidence that hydride can exist in small quantities together with hydroxide in an apatite structure.[26] The presence of hydride in proton conductors such as Al-doped $SrTiO_3$ has also been speculated upon.[32,33] Other related exotic forms of hydrogen in a titanate perovskite lattice have also been examined theoretically.[34−37] In these papers, the stability of interstitial protons, $H^-$ at anionic sites, and $H_2$ molecules bound to Ti has been discussed. There is much speculation on the various exotic forms hydrogen can take in an oxide matrix, and this multistep anion manipulation may offer one experimental route to such systems.

## ■ CONCLUSIONS

With these three experiments, we show how the oxyhydride $BaTiO_{2.5}H_{0.5}$ can lead to exotic compounds and unusual reactivity. Oxyhydrides markedly differ from oxides and other mixed anion systems given the hydride's thermolability and reactivity with acids/oxidizer agents. The formation of an oxynitride from $N_2$ as opposed to $NH_3$ at 400 °C is one clear example. Thus, they serve as convenient precursors for reactions and compounds that were previously unobtainable. Here we only examine the use of one oxyhydride, but perovskite-type oxyhydrides are rapidly expanding in scope in the recent years,[5−9] and hence there will be more room to explore the use of oxyhydrides as precursors in solid state chemistry. We believe our multistep anion exchange can serve as a promising route with continued efforts.

## ■ ASSOCIATED CONTENT

### Supporting Information

The Supporting Information is available free of charge on the ACS Publications website at DOI: 10.1021/jacs.5b10255.

TEM images of $BaTiO_3$, $CaD_2$ synthesis, and crystallographic information on $BaTiO_{2.7}H_{0.15}F_{0.15}$ (PDF)

## ■ AUTHOR INFORMATION


### Corresponding Authors

*yojik@scl.kyoto-u.ac.jp

*kage@scl.kyoto-u.ac.jp



### Funding

This work was supported by Core Research for Evolutional Science and Technology (CREST) from the Japan Science and Technology Agency (JST), a Japan−France Bilateral Joint Research Project from the Japan Society for the Promotion of Science (JSPS), and the Centre National de la Recherche Scientifique (CNRS), PRC No. 0684 2013−2014.


### Notes

The authors declare no competing financial interest.

## ■ ACKNOWLEDGMENTS


We acknowledge beam time awarded from JASRI at SPring-8 (Proposals 2013B1117 and 2014A1465), from ILL (Experiment No. 5-22-722), and from ANSTO (Proposal No. P2764). We are also grateful to C.R. for additional beam time.


## ■ REFERENCES


(1) Kim, Y.-I.; Woodward, P. M.; Baba-Kishi, K. Z.; Tai, C. W. *Chem. Mater.* **2004**, *16*, 1267−1276.

(2) Ai-Mamouri, M.; Edwards, P. P.; Greaves, C.; Slaski, M. *Nature* **1994**, *369*, 382−384.

(3) Ishikawa, A.; Takata, T.; Kondo, J. N.; Hara, M.; Kobayashi, H.; Domen, K. *J. Am. Chem. Soc.* **2002**, *124*, 13547−13553.




DOI: 10.1021/jacs.5b10255
*J. Am. Chem. Soc.* 2015, 137, 15315−15321

(4) Hayward, M. A.; Cussen, E. J.; Claridge, J. B.; Bieringer, M.; Rosseinsky, M. J.; Kiely, C. J.; Blundell, S. J.; Marshall, I. M.; Pratt, F. L. *Science* **2002**, *295*, 1882−1884.
(5) Kobayashi, Y.; Hernandez, O. J.; Sakaguchi, T.; Yajima, T.; Roisnel, T.; Tsujimoto, Y.; Morita, M.; Noda, Y.; Mogami, Y.; Kitada, A.; Ohkura, M.; Hosokawa, S.; Li, Z.; Hayashi, K.; Kusano, Y.; Kim, J. e.; Tsuji, N.; Fujiwara, A.; Matsushita, Y.; Yoshimura, K.; Takegoshi, K.; Inoue, M.; Takano, M.; Kageyama, H. *Nat. Mater.* **2012**, *11*, 507−511.
(6) Sakaguchi, T.; Kobayashi, Y.; Yajima, T.; Ohkura, M.; Tassel, C.; Takeiri, F.; Mitsuoka, S.; Ohkubo, H.; Yamamoto, T.; Kim, J. E.; Tsuji, N.; Fujihara, A.; Matsushita, Y.; Hester, J.; Avdeev, M.; Ohoyama, K.; Kageyama, H. *Inorg. Chem.* **2012**, *51*, 11371−11376.
(7) Denis Romero, F.; Leach, A.; Möller, J. S.; Foronda, F.; Blundell, S. J.; Hayward, M. A. *Angew. Chem., Int. Ed.* **2014**, *53*, 7556−7559.
(8) Bang, J.; Matsuishi, S.; Hiraka, H.; Fujisaki, F.; Otomo, T.; Maki, S.; Yamaura, J.; Kumai, R.; Murakami, Y.; Hosono, H. *J. Am. Chem. Soc.* **2014**, *136*, 7221−7224.
(9) Tassel, C.; Goto, Y.; Kuno, Y.; Hester, J.; Green, M.; Kobayashi, Y.; Kageyama, H. *Angew. Chem., Int. Ed.* **2014**, *53*, 10377−10380.
(10) Bridges, C. a.; Fernandez-Alonso, F.; Goff, J. P.; Rosseinsky, M. J. *Adv. Mater.* **2006**, *18*, 3304−3308.
(11) Jorge, A. B.; Oró-Solé, J.; Bea, A. M.; Mufti, N.; Palstra, T. T. M.; Rodgers, J. A.; Attfield, J. P.; Fuertes, A. *J. Am. Chem. Soc.* **2008**, *130*, 12572−12573.
(12) Bräuniger, T.; Müller, T.; Pampel, A.; Abicht, H.-P. *Chem. Mater.* **2005**, *17*, 4114−4117.
(13) Hitoki, G.; Takata, T.; Kondo, J. N.; Hara, M.; Kobayashi, H.; Domen, K. *Chem. Commun.* **2002**, 1698−1699.
(14) Yajima, T.; Takeiri, F.; Aidzu, K.; Akamatsu, H.; Fujita, K.; Yoshimune, W.; Ohkura, M.; Lei, S.; Gopalan, V.; Tanaka, K.; Brown, C. M.; Green, M. A.; Yamamoto, T.; Kobayashi, Y.; Kageyama, H. *Nat. Chem.* **2015**, DOI: 10.1038/nchem.2370.
(15) Endo, T.; Kobayashi, T.; Sato, T.; Shimada, M. *J. Mater. Sci.* **1990**, *25*, 619−623.
(16) Izumi, F.; Momma, K. *Solid State Phenom.* **2007**, *130*, 15−20.
(17) Rodríguez-Carvajal, J. *Phys. B* **1993**, *192*, 55−69.
(18) Izumi, F.; Dilanian, R. A. Structure refinement based on the maximum-entropy method from powder diffraction data. In *Recent Research Developments in Physics*; Pandalai, S. G., Ed.; **2002**; Vol. *3*, Part II.
(19) Momma, K.; Izumi, F. *J. Appl. Crystallogr.* **2011**, *44*, 1272−1276.
(20) Ruan, G.; Xu, H.; Zhang, Z.; Yin, M.; Xu, G.; Zhan, X. *J. Am. Ceram. Soc.* **2013**, *96*, 1706−1708.
(21) Cheviré, F.; Pallu, A.; Ray, E.; Tessier, F. *J. Alloys Compd.* **2011**, *509*, 5839−5842.
(22) Rhein, R. A. *Lithium Combustion: A Review*; Naval Weapons Center: China Lake, CA, 1990.
(23) Zong, F.; Meng, C.; Guo, Z.; Ji, F.; Xiao, H.; Zhang, X.; Ma, J.; Ma, H. *J. Alloys Compd.* **2010**, *508*, 172−176.
(24) McDonald, N. R.; Wallwork, G. R. *Oxid. Met.* **1970**, *2*, 263−283.
(25) Coufová, P.; Novák, J.; Hlasivcová, N. *J. Chem. Phys.* **1966**, *45*, 3171−3174.
(26) Hayashi, K.; Sushko, P. V; Hashimoto, Y.; Shluger, A. L.; Hosono, H. *Nat. Commun.* **2014**, *5*, 3515.
(27) Nagasaki, T.; Shiotani, S.; Igawa, N.; Yoshino, M.; Iwasaki, K.; Fukazawa, H.; Utsumi, W. *J. Solid State Chem.* **2009**, *182*, 2632−2639.
(28) Norberg, S. T.; Rahman, S. M. H.; Hull, S.; Knee, C. S.; Eriksson, S. G. *J. Phys.: Condens. Matter* **2013**, *25*, 454214.
(29) Ahmed, I.; Knee, C. S.; Karlsson, M.; Eriksson, S.-G.; Henry, P. F.; Matic, A.; Engberg, D.; Börjesson, L. *J. Alloys Compd.* **2008**, *450*, 103−110.
(30) Sata, N.; Hiramoto, K.; Ishigame, M.; Hosoya, S.; Niimura, N.; Shin, S. *Phys. Rev. B: Condens. Matter Mater. Phys.* **1996**, *54*, 15795−15799.
(31) Schouwink, P.; Ley, M. B.; Tissot, A.; Hagemann, H.; Jensen, T. R.; Smrčok, L.; Černý, R. *Nat. Commun.* **2014**, *5*, 5706.
(32) Widerøe, M.; Münch, W.; Larring, Y.; Norby, T. *Solid State Ionics* **2002**, *155*, 669−677.
(33) Norby, T.; Widerøe, M.; Glöckner, R.; Larring, Y. *Dalt. Trans.* **2004**, 3012−3018.
(34) Iwazaki, Y.; Suzuki, T.; Tsuneyuki, S. *J. Appl. Phys.* **2010**, *108*, 83705.
(35) Iwazaki, Y.; Gohda, Y.; Tsuneyuki, S. *APL Mater.* **2014**, *2*, 012103.
(36) Varley, J. B.; Janotti, A.; Van de Walle, C. G. *Phys. Rev. B: Condens. Matter Mater. Phys.* **2014**, *89*, 075202.
(37) Zhang, J.; Gou, G.; Pan, B. *J. Phys. Chem. C* **2014**, *118*, 17254−17259.


DOI: 10.1021/jacs.5b10255
*J. Am. Chem. Soc.* 2015, 137, 15315−15321